J. Membrane Biol. 118, 171–178 (1990)

The Journal of
Membrane Biology

Multiple Conductance Levels of the Dihydropyridine-Sensitive Calcium Channel in GH_3 Cells

Diana L. Kunze† and Aileen K. Ritchie‡

†Department of Physiology and Molecular Biophysics, Baylor College of Medicine, Houston, Texas 77030, and
‡Department of Physiology and Biophysics, University of Texas Medical Branch, Galveston, Texas 77550

Summary. Calcium channels in GH_3 cells exhibit at least five conductance levels when examined in cell-attached or outside-out patches. These channels resemble the high threshold Ca^{2+} current in their range of activation and inactivation, and in their sensitivity to dihydropyridines (DHP). Mean open times for the five levels were brief (<1 msec) in control solutions but increased in the presence of BAY K 8644. In 100 mM Ba^{2+} and BAY K 8644, the five predominant slope conductances were 8–9, 12–13, 16–18, 23–24, and 28 pS. The present study is the first report of multiple levels of the DHP-sensitive Ca^{2+} channel occurring with high frequency in native membranes. The range of conductance levels that we observed encompasses the range of conductances found for two other different types of Ca^{2+} channels and indicates that unit conductance should be used with caution as a distinguishing characteristic for identification of different channel types.

Key Words calcium channel · dihydropyridines · subconductances · single channels · anterior pituitary cells

Introduction

A number of different types of voltage-dependent Ca^{2+} channels are known to coexist in neurons, cardiac cells, and endocrine cells. Much attention has been placed on the distinguishing characteristics of the channels and their relationship to functional properties such as transmitter release, neuronal growth, and spontaneous electrical activity. A Ca^{2+} channel that has a relatively high activation threshold, exhibits a sustained current under whole-cell voltage clamp, and is sensitive to inhibition by the dihydropyridines (DHP), is often referred to as the L-type channel (LLinas & Yarom, 1981; Nowycky, Fox & Tsien, 1985*b*; *also see* for review, Tsien et al., 1988). This DHP-sensitive channel is a major pathway for spontaneous and stimulus-evoked influx of Ca^{2+} in the GH_3 anterior pituitary cell line (Cohen & McCarthy, 1987). The GH_3 cell also has a T-type Ca^{2+} channel that is DHP insensitive, low threshold, and rapidly inactivating (Matteson & Armstrong, 1986; Cohen & McCarthy, 1987). A third N-type channel (Nowycky et al., 1985*b*) with high activation threshold, moderately rapid inactivation kinetics, and an insensitivity to DHP, does not appear to be present (Cohen & McCarthy, 1987; D.L. Kunze & A.K. Ritchie, *unpublished observations*).

One of the criteria that has evolved for classifying the different types of Ca^{2+} channels has been the amplitude of the single-channel currents. In contrast to most previously reported studies of the L-type Ca^{2+} channel in native membranes, including those with GH_3 cells (Hagiwara & Ohmori, 1983; Armstrong & Eckert, 1987), we find that the DHP-sensitive channel in GH_3 cells exists, not as a channel of single unitary amplitude, but one that exhibits a minimum of five different conductances. This work reinforces the need to carefully examine channel characteristics other than amplitude as a criterion for classification of multiple channel types. Although the mechanisms responsible for the appearance of the particular conductance levels is as yet unknown, the potential for regulation of calcium influx by manipulation of the state of the channel exists. Finally this work will be of interest to those researchers interested in the structure-function relationship of ion permeation. A preliminary account of these studies has been previously reported (Kunze & Ritchie, 1989).

Materials and Methods

The GH_3 cell line was obtained from the American Type Culture Collection (Rockville, MD). The cells were maintained at 37°C and 5% CO_2 in HAM's F10 medium containing 15% heat-inactivated horse serum and 2.5% fetal calf serum. The cells were used for electrophysiological recording 1–10 days after plating. Similar solutions were used for whole-cell recording and for recording

single channels from outside-out patches. The pipette contained (in mM): 105 N-methyl-D-glucamine (NMDG), 110 aspartic acid, 15 ethylene glycol *bis*-(β-aminoethyl ether) N,N,N′,N′-tetraacetic acid (EGTA), 5 [1,2-*bis*(2-aminophenoxy) ethane-N,N,N′,N′-tetraacetic acid] (BAPTA), 10 N-2-hydroxyethyl piperazine-N′2-ethane sulfonic acid (HEPES), 2.5 $MgCl_2$, with adjustment to pH 7.2 with CsOH (solution A). In addition, 0.5 theophylline bromide, 1.6 ATP, 0.1 cAMP and 0.1 to 1 GTP were often included to help stabilize the currents. In a few instances the pipette solution used to record from outside-out patches contained (in mM): 124 CsCl, 11 EGTA, 1 $CaCl_2$, 2 $MgCl_2$ and 10 HEPES, pH 7.2 (solution B). The bathing solution contained 100 $BaCl_2$ and 10 HEPES, with pH adjusted to 7.2 with BaOH or KOH (solution C). The latter solution was also used in the pipette for single-channel recordings from cell-attached patches. The bathing solution, when recording from cell-attached patches, contained (in mM): 140 KAspartate (KAsp), 10 EGTA, 10 HEPES and 1 $MgCl_2$, pH adjusted to 7.4 with KOH (solution D). (±) BAY K 8644 and nimodipine were kindly supplied by A. Scriabine of Miles Laboratories, West Haven, CT. All experiments were performed at room temperature.

Patch pipettes of 3–10 MΩ resistance were prepared from thin wall borosilicate glass (WPI) or 7052 or 8161 glass (Garner Glass). Pipettes were fire polished and, in some instances, coated with Sylgard. The ground electrode was a silver-silver chloride pellet connected to the bath via a KCl agar bridge. Potential differences between the recording pipette and the bath ground were nullified prior to seal formation. Data were recorded using the List EPC7 patch-clamp amplifier. Voltages that are reported have been corrected for the liquid junction potential (ljp). The ljp was measured as the potential difference between the recording solution and the bath solution after the two solutions were connected via a KCl agar bridge. A correction of −13 mV was required when the bath contained 100 mM $BaCl_2$ and NMDG-Aspartate solution was in the recording electrode. No correction was applied when using 100 mM $BaCl_2$ in the pipette and KAsp in the bath since the ljp between these two solutions was only 1 mV.

The whole-cell data were stored on FM tape. The data were analyzed manually after playback at a sevenfold slower speed onto a Gould strip chart recorder or by computer after digitization. The single-channel data were analog filtered at a cutoff frequency of 5–10 kHz (4-pole Bessel Filter, −3 dB; Wavetek, San Diego, CA) and digitized on-line at 10–20 kHz. A 4-pole zero phase digital filter was used during the analysis for further filtering. Data were analyzed using a threshold, half-amplitude method (Lux & Brown, 1984). Amplitude histograms were constructed either from the idealized data (*see* Fig. 2, the Table) or from all data points (*see* Fig. 4). All current traces, whole cell and single channel, are illustrated with negative current (positive charges moving from the extracellular to intracellular side of the membrane) in the downward direction. All voltages are reported relative to the extracellular side of the membrane.

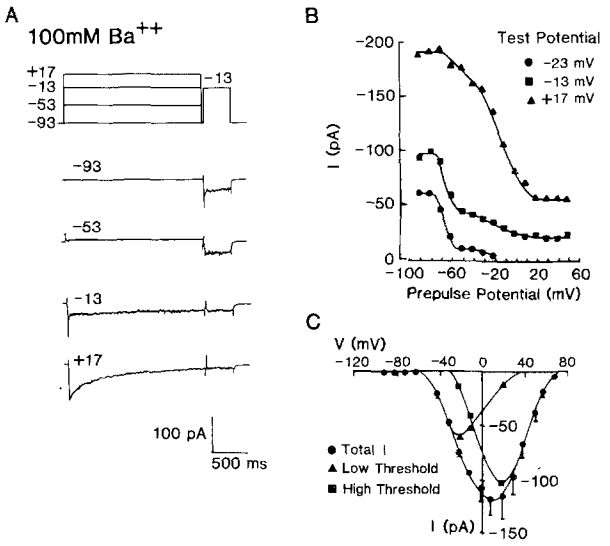

Fig. 1. Whole-cell recording in 100 mM Ba^{2+}. (*A*) Examples of current traces in response to a 400-msec voltage step to −13 mV from a holding potential of −93 mV, with or without 1-sec prepulses to the indicated potentials. Leakage current has not been subtracted from the current traces. (*B*) Effect of prepulse potentials of 1-sec duration on test pulses to −13, −23 and +17 mV. A linear leakage current has been subtracted from the current amplitudes. (*C*) The circles represent the mean peak amplitudes measured upon stepping to the indicated potentials. The error bar indicates SEM for three determinations made in the same cell. The low threshold component of current (triangles) was determined as the portion of the total current that was inactivated by prepulses to −53 mV. These were determined for the three test potentials illustrated in *B* above. The currents evoked by the two test potentials more negative than −23 mV were also abolished by prepulses to −53 mV. The remainder of the current is represented as the high threshold component (squares). Recordings were made with solutions A (pipette) and C (bath).

Results

Properties of the Whole-Cell Current

The voltage- and time-dependent properties of the whole-cell currents were examined in order to design the protocols for the single-channel studies. In whole-cell voltage-clamp recording with 100 mM barium as the ion-carrying species, a voltage step to −13 mV from a holding potential of −93 mV shows a rapidly inactivating and a slowly inactivating component (Fig. 1*A*). The rapidly inactivating component was eliminated by a 1-sec prepulse to −53 mV and the slowly decaying component was partially inactivated by 1-sec prepulses in the voltage range between −40 and +20 mV (Fig. 1*A* and *B*, squares). In the prepulse step to +17 mV, a portion of the high threshold current can be seen to inactivate with a moderately rapid time course, but slower than inactivation of the low threshold current. A plot of the total current activated at different step potentials is shown in Fig. 1*C*, circles. The rapidly inactivating component of current that is eliminated by prepulses to −53 mV is indicated by the triangles. This low threshold, or T-type channel, activates around −53 and peaks around −20 mV. The high threshold, or L-type, current (squares), plotted as the fraction of total current that remains after prepulses to −53

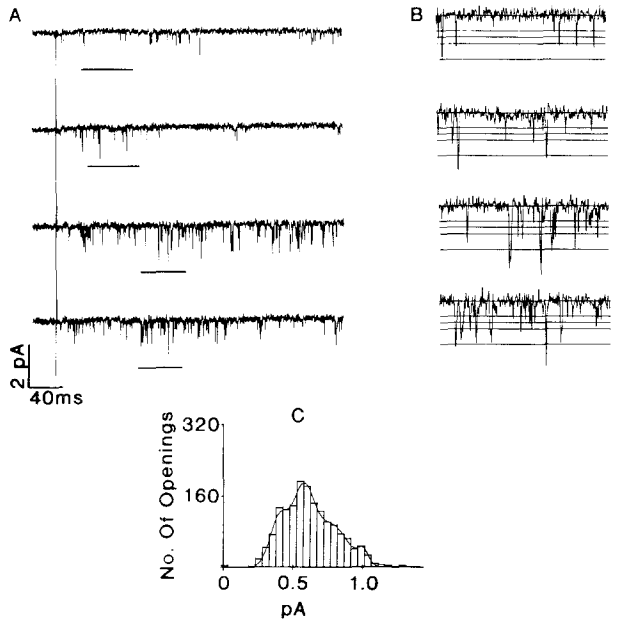

Fig. 2. Channel activity in a cell-attached patch. Depolarizing pulses of 300-msec duration were applied every 6 sec to 0 mV from a holding potential of −40 mV. Representative traces are shown in (*A*) with a portion of each trace shown on an expanded time scale in (*B*). The lines are the values for the mean amplitudes obtained for a multiple Gaussian fit to the single-channel amplitude histogram (*C*) for this patch (1747 openings). The amplitude histogram was constructed from idealized data, as described in Materials and Methods. Data were filtered at 2.5 kHz for amplitude analyses and at 1 kHz for illustration. Recordings were made with solutions C (pipette) and D (bath).

mV, activates around −20 and peaks at +20 mV. In agreement with others, we have found that DHP antagonists (nimodipine) and agonists (BAY K 8644), when used at a concentration of 1 μM or less, respectively inhibit or amplify the high threshold current, while the low threshold current is DHP insensitive. Higher concentrations of the DHP compounds are known to act in a nonselective manner (Hume, 1985; Yatani & Brown, 1985; Akaike, Kostyuk & Osipchuk, 1989).

The above described properties were used to determine the requisite conditions needed to study single high threshold channels in membrane patches without contamination from low threshold channels. This was achieved by holding the patch at, or more positive than, −40 mV.

Single-Channel Activity in Control Patches that Were Not Exposed to BAY K 8644

In the cell-attached mode the cells were bathed in 140 mM KAsp to bring the membrane potential to 0 mV. Depolarizing pulses from a holding potential of −40 mV were applied to elicit channel activity (Fig. 2). The activity appeared as brief openings with amplitudes of various sizes. Expanded portions of the records are shown in the same figure. Several sizes were evident initially in each patch although the largest sizes were rare. The amplitude histogram from this patch was not well fitted by a single Gaussian distribution. The best fit, obtained by minimization of the Chi square value, was the sum of four Gaussian distributions with mean amplitudes of 0.39, 0.57, 0.77 and 1.0 pA. The fifth and largest conductance channel appeared so infrequently that its contribution to the amplitude histogram was minimal. The table gives the amplitudes obtained from multiple Gaussian fits of activity of seven patches at 0 mV. The various amplitudes could appear as the result of frequency limitations of the recording method; however, the non-unimodal distribution of the amplitude histogram suggested the additional possibility of multiple conductance levels.

Table.

	a	b	c	d	f
Amplitude	0.42 ± 0.06 $n = 7$	0.60 ± 0.04 $n = 6$	0.82 ± 0.03 $n = 7$	1.03* $n = 2$	1.49* ± 0.08 $n = 5$

Single-channel amplitudes (in pA) are given as the mean ± SD with n = the number of patches. Not all of the patches contained all five amplitudes.
* Average of measurement of 5–15 openings in each patch. All others are the mean of Gaussian fit to amplitude histogram data.

Inhibition of Single-Channel Activity by Nimodipine

In addition to the high threshold, L-type, DHP-sensitive Ca^{2+} channel, two other types of DHP-insensitive Ca^{2+} channels (types T and N) coexist in dorsal root ganglion cells (Nowycky, Fox & Tsien, 1985*a*; Kostyuk, Shuba & Savchenko, 1988), and the T-type channel has been reported for GH_3 cells (Kunze & Ritchie, 1986; Armstrong & Eckert, 1987). Because these other channel types exhibit smaller amplitudes than the L-type when carrying Ba^{2+} current, we wished to determine if all of the amplitudes that we observed were DHP sensitive. Figure 3 contains examples of channel activity in a cell-attached patch where different amplitude levels can be seen more clearly by the occasional presence of long duration channel openings. The Gaussian fits to the amplitude histogram gave values of 0.52, 0.76, 1.02, and 1.46 pA. Application of nimodipine (100 nM) for 6 sec (Fig. 3) caused cessation of all activity. As the

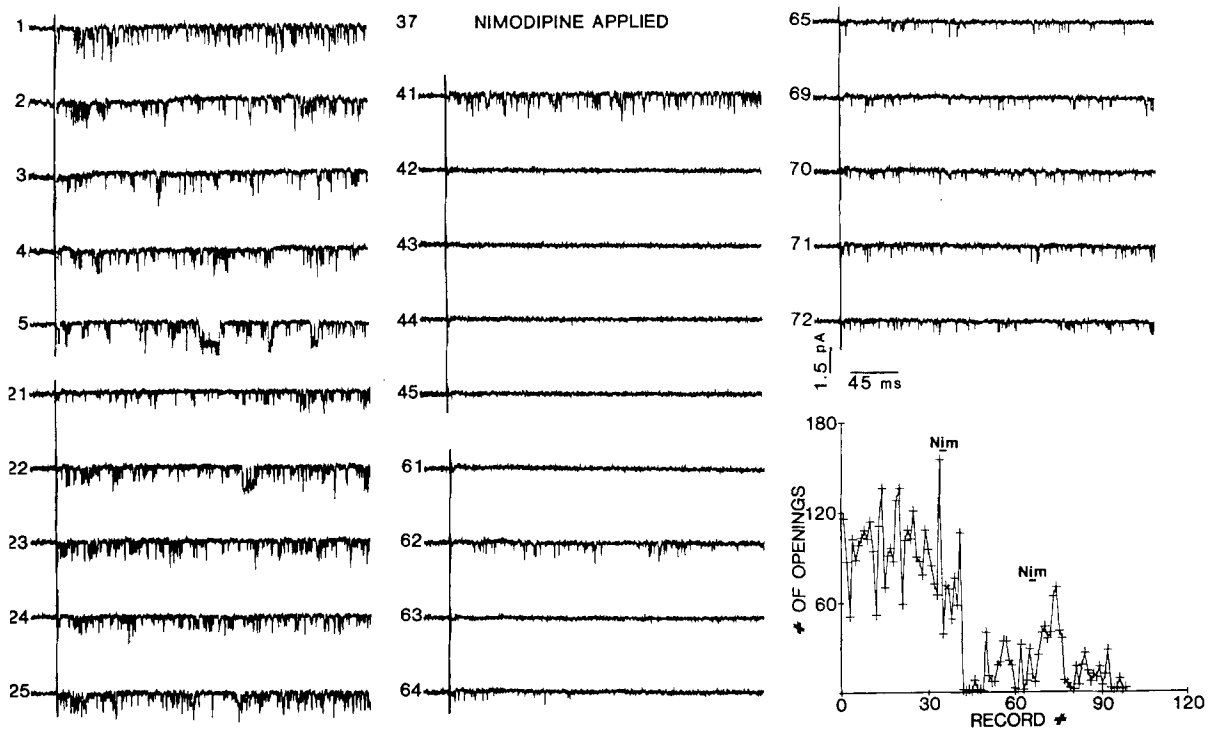

Fig. 3. Effect of nimodipine on channel activity in a cell-attached patch. The data were recorded during voltage steps to 0 mV from a holding potential of −40 mV. The record number is indicated to the left of each trace. Five consecutive traces are displayed every 20 records until the application of nimodipine. Traces in the center panel were recorded after nimodipine was applied at record number 38 as a 6-sec pulse. The number of openings *vs.* the record number is plotted in the lower part of the figure. Activity returned following the application of nimodipine (indicated by bar). The drug was applied a second time when the activity began to recover. Similar results were obtained in three other patches. Data were filtered at 1 kHz for illustration. Recordings were made with solutions C (pipette) and D (bath).

nimodipine washed away, some channel activity was restored. This shows that the different amplitudes are all DHP sensitive and thus do not represent contamination by N- or T-type channels.

BAY K 8644 Treated Channels

In order to show more clearly that the different channel amplitudes that were observed in control patches represent different conductance states and not differences in frequency clipping, we recorded channel activity in the presence of BAY K 8644. This Ca^{2+} channel agonist is known to cause selective prolongation of the DHP-sensitive channel. In the experiment shown in Fig. 4*A*, the patch potential was held constant at −10 mV. At the beginning of the trace, channel activity consisted of brief spikes of various amplitudes. In response to a 20-sec pressure application of 300 nM (±) BAY K 8644, single-channel open times were prolonged and the multiple amplitude levels were more readily apparent. In this patch at least three different conductance levels can be seen opening and closing from the baseline (Fig. 4*B*, expanded traces). Openings from baseline to several other current levels were also present but occurred less frequently. In addition, openings of different amplitude often occurred from levels other than baseline, and the largest unitary amplitude was often found superimposed on another opening of similar large size. This suggests that more than one channel was present in this patch. The different conductance levels, opening from baseline, can be seen more clearly when holding at −20 mV where the opening probability is lower (Fig. 4*C*). The three predominant conductance levels can also be seen in the amplitude histogram for this patch at −20 mV (Fig. 4*D*). The current-voltage relationships for this patch are plotted at four potentials (Fig. 4*E*). Slope conductances of 8, 12 and 28 pS were determined for the three most frequently observed levels.

Single-channel activity from an excised patch in the outside-out configuration is shown in Fig. 5. This patch exhibited three predominant amplitudes. The amplitudes for which slope conductances could be measured were 12 and 23 pS. Although all patches exhibited at least three conductance levels, the lev-

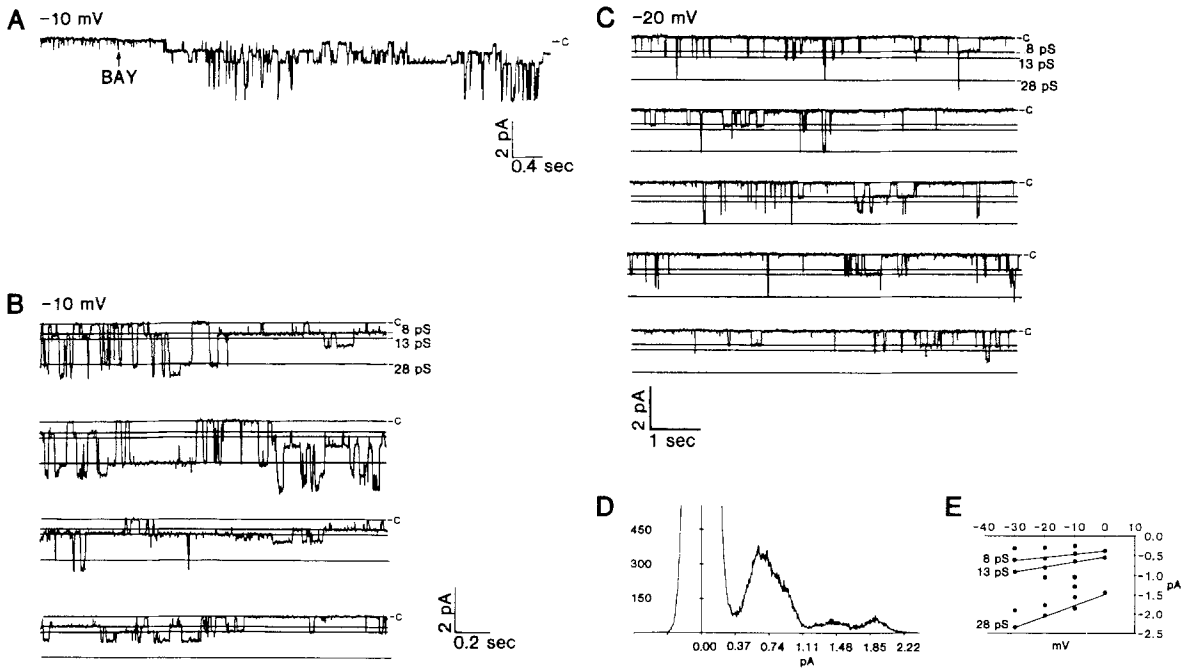

Fig. 4. Effect of BAY K 8644 on channel activity in a cell-attached patch. (*A*) The patch potential was held at −10 mV and 300 nM. BAY was superfused at the arrow for 20 sec using pressure application from a pipette placed in close proximity (10–15 μm) to the cell. (*B*) Traces selected from recordings made after the application of BAY K 8644 are shown on an expanded time scale to illustrate the different current levels in the patch. The lines represent the major current amplitudes for openings from the closed state. (*C*) Activity in the same patch at −20 mV. (*D*) The amplitude histogram for channel activity at −20 mV. The initial truncated peak represents the distribution of baseline noise. The second peak with the shoulder represents the 8- and 13-pS sized channels. The third peak, distributed around 1.48 pA, represents multiple hits of the two previously mentioned amplitudes. The fourth peak, distributed around 1.95 pA, represents the 28-pS channel. (*E*) The current-voltage relationships for the different amplitudes in this patch are shown at potentials from −30 to 0 mV. The major conductance levels are shown with linear least-squares fits to the amplitudes. Data were filtered at 1 kHz for amplitude analyses and 200 Hz for illustration. Recordings were made with solutions C (pipette) and D (bath)

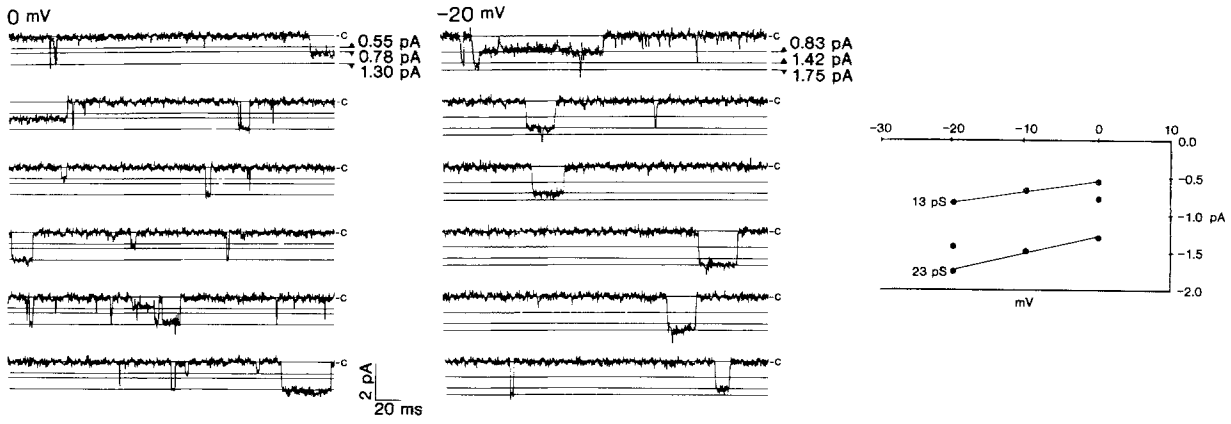

Fig. 5. Examples of activity from an outside-out patch following pressure application of 500 nM BAY K 8644. The lines are amplitude levels of the three predominant sizes at 0 and −20 mV. The current-voltage relationship for this patch reveals conductances of 13 and 23 pS for the smallest and largest amplitude channels. However, the predominant amplitude of the middle sized channel seen at 0 mV is apparently of a different conductance than that which occurs at −20 mV. Data were filtered at 1 kHz for illustration. Recordings were made with solutions A (pipette) and C (bath)

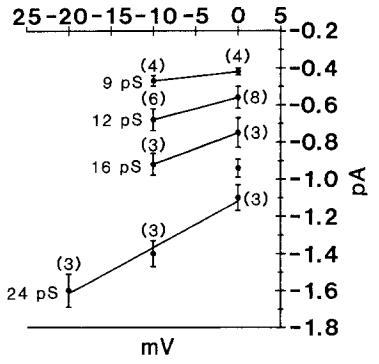

Fig. 6. The current-voltage relationships of single-channel amplitudes obtained in the presence of 100 to 500 nM BAY K 8644. The majority of amplitudes were determined from Gaussian fits to data obtained from a total of 18 patches (cell attached or outside-out). When the number of openings of the large amplitude sizes was insufficient to construct a histogram, the amplitude was determined from the mean of direct measurements of 5 to 15 openings. Most of the patches (n = 14) were studied by using 200–300 msec voltage steps to −20, −10 and/or 0 mV from a holding potential of −40 or −30 mV. Four of the patches were studied while holding at the indicated voltages. The points represent the mean ± SD of amplitudes obtained from individual patches

els that were observed were not always the same in the different patches.

Comparable data have been obtained from a total of 18 patches where channel activity was recorded at either a constant voltage of 0 or −10 mV (n = 4) or during a voltage step protocol (n = 14) to 0 or −10 mV from holding potentials of −40 or −30 mV. BAY K 8644 was added to the bath at concentrations of 100 to 500 nM. Any one patch showed at least three to four different conductance levels initially, although after several minutes some of the levels disappeared. The disappearance was also accompanied by a decrease in open probability and a decrease in the occurrence of multiple openings that we ascribe to the phenomena of run-down (Armstrong & Eckert, 1987; Belles et al., 1988). Patches containing channels of single unitary amplitude were not observed. The mean amplitude values, obtained from the best fit of amplitude histograms to multiple Gaussian distributions, are plotted in Fig. 6. The major conductances, determined from the slope of the mean amplitudes, were 9, 12, 16, and 24 pS. Other levels were less frequently seen. The predominant conductance in 7 of the 14 patches where voltage steps were used was the 12–13 pS range, and in 5 of the patches, the 16–18 pS range. Transitions from one amplitude to another were occasionally evident (*see* Fig. 5). However, the majority of the openings appeared from a closed state or as superpositions on other openings. Nimodipine also reversibly blocked all channel activity in BAY K 8644 treated patches that showed activity of different amplitudes (*data not shown*).

Discussion

In this study we show that the high threshold, DHP-sensitive Ca^{2+} channel in intact GH_3 cells exhibits at least five different conductance levels (8–9, 12–13, 16–18, 23–24 and 28 pS). Multiple levels can be seen in the absence of BAY K 8644; however, they are more convincing in the presence of the agonist which increases the mean open time of all conductance levels. We do not know if the different conductance levels that we see within a patch represent stable conformational states of different channels in the patch, a single channel undergoing rapid transitions to different conductance levels, or channels of a single unitary amplitude that aggregate then gate coincidentally (Fox, 1987; Patlak, 1988; Meves & Nagy, 1989). The presence of at least three conductance levels in nearly every patch that we examined and frequent superimpositions of these levels precluded further statistical analyses to distinguish between independent openings, cooperative openings or transitions to different substates.

Except for a few isolated examples (Chen & Hess, 1988; Lacerda & Brown, 1989), the DHP-sensitive Ca^{2+} channel that has been recorded in membrane patches is usually observed as a channel of single unitary amplitude. In a wide variety of cell types, including cardiac cells (Reuter et al., 1982; Cavalie et al., 1983), dorsal root ganglion cells (Nowycky et al., 1985*a*), pancreatic beta cells (Rorsman, Ashcroft & Trube, 1988), and the RINm5F insulin-secreting cell line (Velasco, Petersen & Petersen, 1988), the unit conductance in 100 mM $BaCl_2$ has been reported to range from 18 to 30 pS. A curious exception is the GH_3 cell for which a conductance of 7 pS has been reported by Hagiwara and Ohmori (1983). This is much smaller than the more commonly reported size (28 pS) found in the same cell line by Armstrong and Eckert (1987).

In contrast to the channel in native membranes, multiple conductance levels are often observed for the calcium channel that has been reconstituted into lipid bilayers. Ma and Coronado (1988) report conductance states of 3, 9 and 12 pS for Ca^{2+} channels that have been incorporated into bilayers from skeletal muscle t-tubule vesicles, while Erlich et al. (1986) found a major conductance of 8 pS, and minor subconductances, in bilayers containing Ca^{2+} channels from cardiac sarcolemmal vesicles. Multiple conductance states have also been observed in bilayers containing the purified DHP receptor protein from skeletal muscle. Smith et al. (1987) report one con-

ductance size of 12–14 pS and another of 22 pS. Talvenheimo, Worley and Nelson (1987) have identified 7- and 16-pS conductances. Finally Hymel et al. (1988) have reported channels as small as 0.9 pS, predominant sizes of 7.5 and 15 pS, but occasional conductances as large as 60 pS. Hymel et al. (1988), suggest that a single channel has a unit conductance of 0.9 pS and that all larger conductance levels represent the coincident gating of parallel conducting channels within an aggregate. Likewise, Ma and Coronado (1988) find that the Ca^{2+} channel in lipid bilayers exists as two different conductances and that a third conductance appears when the two aggregate channels open and close in a concerted fashion.

In GH_3 cells there are at least five predominantly occurring conductance levels. Because the levels are close together, it is possible that the channel can actually assume a continuum of conductance levels within the observed range. Alternatively, the levels may represent discrete levels, in which case, they appear to be multiples of a single unitary amplitude channel of 4 pS, with some ambiguity in the size of the channel or channels between the 16- and 24-pS sizes. We see interconversions between the different levels; however, their occurrence is rare. If the larger size openings represent aggregates of channels that open and close coincidentally, then they are stable aggregates because the different conductance levels are usually observed as apparent superimpositions on other openings or as openings from the baseline.

The appearance of multiple conductance levels in GH_3 cells, in our hands, occurred in nearly every patch that was analyzed. It is, therefore, somewhat puzzling that other than a few exceptions (Chen & Hess, 1988; Lacerda & Brown, 1989), multiple levels have not been observed in native membranes. It is possible that the appearance of different conductance levels is influenced by the nutritional state of the cell. Since the activity of the DHP-sensitive Ca^{2+} channel is known to be influenced by phosphorylation (Rane & Dunlap, 1986; Armstrong & Eckert, 1987; Trautwein et al., 1987) and by G proteins (Imoto et al., 1988; Yatani et al., 1988), we are presently attempting to determine if either influences the appearance of multiple levels or favors a particular conductance level. This may account for the wide disparity in channel conductance that has been reported for the Ca^{2+} channel in GH_3 cells.

We wish to thank C. Roberson and J.D. Bond for preparing the illustrations and Drs. John Dani, Antonio Lacerda and Enrico Stefani for helpful criticisms of the manuscript. This work was supported by NIH grants NS23573 (DLK) and DK33898 (AKR).

References

Akaike, N., Kostyuk, P.G., Osipchuk, Y.V. 1989. Dihydropyridine-sensitive low-threshold calcium channels in isolated rat hypothalamic neurones. *J. Physiol. (London)* **412:**181–195

Armstrong, D., Eckert, R. 1987. Voltage-activated calcium channels that must be phosphorylated to respond to membrane depolarization. *Proc. Natl. Acad. Sci. USA* **84:**2518–2522

Belles, B., Malecot, C.O., Hescheler, J., Trautwein, W. 1988. "Rundown" of the Ca current during long whole-cell recordings in guinea pig heart cells: Role of phosphorylation and intracellular calcium. *Pfluegers Arch.* **411:**353–360

Cavalie, A., Ochi, R., Pelzer, D., Trautwein, W. 1983. Elementary currents through Ca^{2+} channels in guinea pig myocytes. *Pfluegers Arch.* **398:**284–297

Chen, C., Hess, P. 1988. A complex new gating pattern detected in L-type calcium channels from guinea-pig ventricular monocytes and mouse 3T3 fibroblasts. *J. Physiol. (London)* **390:**80P

Cohen, C.J., McCarthy, R.T. 1987. Nimodipine block of calcium channels in rat anterior pituitary cells. *J. Physiol. (London)* **387:**195–225

Erlich, B.E., Schen, C.R., Garcia, M.L., Kaczorowski, G.J. 1986. Incorporation of calcium channels from cardiac sarcolemmal membrane vesicles into planar lipid bilayers. *Proc. Natl. Acad. Sci. USA* **83:**193–197

Fox, J.A. 1987. Ion channel subconductance states. *J. Membrane Biol.* **97:**1–8

Hagiwara, S., Ohmori, H. 1983. Single calcium channel currents in rat clonal pituitary cells. *J. Physiol. (London)* **336:**649–661

Hume, J.R. 1985. Comparative interactions of organic Ca^{++} channel antagonists with myocardial Ca^{++} and K^+ channels. *J. Pharmacol. Exp. Ther.* **234:**134–140

Hymel, L., Striessnig, J., Glossman, H., Schindler, H. 1988. Purified skeletal muscle 1,4-dihydropyridine receptor forms phosphorylation-dependent oligomeric calcium channels in planar bilayers. *Proc. Natl. Acad. Sci. USA* **85:**4290–4294

Imoto, Y., Yatani, A., Reeves, J.P., Codina, J., Birnbaumer, L., Brown, A.M. 1988. α-subunit of Gs directly activates cardiac calcium channels in lipid bilayers. *Am. J. Physiol.* **255:**H722–H728

Kostyuk, P.G., Shuba, Y.M., Savchenko, A.N. 1988. Three types of calcium channels in the membrane of mouse sensory neurons. *Pfluegers Arch.* **411:**661–669

Kunze, D.L., Ritchie, A.K. 1986. Single channel calcium and barium currents in the GH3 cell line. *Biophys. J.* **49:**176*a*

Kunze, D.L., Ritchie, A.K. 1989. Multiple conductance states of the dihydropyridine (DHP) sensitive calcium channel in GH_3 cells. *Biophys. J.* **55:**299*a*

Lacerda, A.E., Brown, A.M. 1989. Nonmodal gating of cardiac calcium channels as revealed by dihydropyridines. *J. Gen. Physiol.* **93:**1243–1273

Llinas, R., Yarom, Y. 1981. Electrophysiology of mammalian inferior olivary neurones in vitro. Different types of voltage-dependent ionic conductances. *J. Physiol. (London)* **315:**549–567

Lux, H.D., Brown, A.M. 1984. Patch and whole cell calcium currents recorded simultaneously in snail neurons. *J. Gen. Physiol.* **83:**727–750

Ma, J., Coronado, R. 1988. Heterogeneity of conductance states in calcium channels of skeletal muscle. *Biophys. J.* **53:**387–395

Matteson, D.R., Armstrong, C.M. 1986. Properties of two types of calcium channels in clonal pituitary cells. *J. Gen. Physiol.* **87:**161–182

Meves, H., Nagy, K. 1989. Multiple conductance states of the

sodium channel and of other ion channels. *Biochim. Biophys. Acta* **988:**99–105

Nowycky, M.C., Fox, A.P., Tsien, R.W. 1985*a*. Long-opening mode of gating of neuronal calcium channels and its promotion by the dihydropyridine calcium agonist Bay K 8644. *Proc. Natl. Acad. Sci. USA* **82:**2178–2182

Nowycky, M.C., Fox, A.P., Tsien, R.W. 1985*b*. Three types of neuronal calcium channel with different calcium agonist sensitivity. *Nature (London)* **316:**440–443

Patlak, J.B. 1988. Sodium channel subconductance levels measured with a new variance-mean analysis. *J. Gen. Physiol.* **92:**413–430

Rane, S.G., Dunlap, K. 1986. Kinase C activator 1,2-oleoylacetylglycerol attenuates voltage-dependent calcium current in sensory neurons. *Proc. Natl. Acad. Sci. USA* **83:**184–188

Reuter, H., Stevens, C.R., Tsien, R.W., Yellen, G. 1982. Properties of single calcium channels in cardiac cell culture. *Nature (London)* **297:**501–504

Rorsman, P., Ashcroft, R.M., Trube, G. 1988. Single Ca channel currents in mouse pancreatic β. *Pfluegers Arch.* **412:**597–603

Smith, J.S., McKenna, E.J., Ma, J., Vilven, J., Vaghy, P.L., Schwartz, A., Coronado, R. 1987. Calcium channel activity in a purified dihydropyridine-receptor preparation of skeletal muscle. *Biochemistry* **26:**7182–7188

Talvenheimo, J.A., Worley, J.F., III, Nelson, M.T. 1987. Heterogeneity of calcium channels from a purified dihydropyridine receptor preparation. *Biophys. J.* **52:**891–899

Trautwein, W., Cavalie, A., Flockerzi, V., Hofmann, F., Pelzer, D. 1987. Modulation of calcium channel function by phosphorylation in guinea pig ventricular cells and phospholipid bilayer membranes. *Circ. Res. (Suppl. I)* **61:**I17–I23

Tsien, R.W., Lipscombe, D., Madison, D.V., Bley, K.R., Fox, A.P. 1988. Multiple types of neuronal calcium channels and their selective modulation. *Trends Neurosci* **11:**431–438

Velasco, J.M., Petersen, J.U.H., Petersen, O.H. 1988. Single-channel Ba^{2+} currents in insulin-secreting cells are activated by glyceraldehyde stimulation. *FEBS Lett.* **231:**366–370

Yatani, A., Brown, A.M. 1985. The calcium channel blocker nitrendipine blocks sodium channels in neonatal rat cardiac myocytes. *Circ. Res.* **56:**868–875

Yatani, A., Imoto, Y., Codina, J., Hamilton, S.L., Brown, A.M., Birnbaumer, L. 1988. The stimulatory G protein of adenylyl cyclase also stimulates skeletal muscle T-tubule Ca^{2+} channels. *J. Biol. Chem.* **263:**9885–9895

Received 6 February 1990; revised 25 April 1990